J Mater Sci: Mater Med (2017) 28:23
DOI 10.1007/s10856-016-5837-8

BIOMATERIALS SYNTHESIS AND CHARACTERIZATION

Original Research

Antibacterial activity and mechanism of Ag/ZnO nanocomposite against anaerobic oral pathogen *Streptococcus mutans*

Shilei Wang[1] · Jie Wu[1] · Hao Yang[1] · Xiangyu Liu[1] · Qiaomu Huang[1] · Zhong Lu[1]

Received: 21 September 2016 / Accepted: 19 December 2016 / Published online: 2 January 2017

Abstract Dental caries is a widespread disease mainly caused by the anaerobic oral pathogen *Streptococcus mutans* (*S. mutans*). Ag/ZnO nanocomposite is an efficient antibacterial agent because of its high antibacterial activity and low cytotoxicity. In this study, rod-like Ag/ZnO nanocomposite was synthesized through a deposition-precipitation method and characterized by X-ray diffraction, scanning electron microscopy and transmission electron microscopy. The activity of Ag/ZnO nanocomposite against *S. mutans* was evaluated by determining the minimal inhibitory concentration, minimum bactericidal concentration and growth inhibition curve. The results showed that Ag/ZnO nanocomposite displayed higher activity against *S. mutans* compared with pure ZnO nanorods. Moreover, the antibacterial mechanism was investigated by determining the bacterial membrane potential, release of K^+, intracellular reactive oxygen generation and lipid peroxidation. Disruption of membrane function and oxidation of biomacromolecules played important role in the antibacterial action of Ag/ZnO nanocomposite. This work proposes a potentially effective dental antibacterial agent against the dental caries-causing *S. mutans*.

✉ Zhong Lu
zhonglu@wit.edu.cn

[1] School of Chemical Engineering and Pharmacy, Key Laboratory for Green Chemical Process of Ministry of Education, Wuhan Institute of Technology, Xiongchu Avenue, Wuhan 430073, PR China

1 Introduction

Dental caries is a progressive, destructive, and infectious disease that is highly prevalent in industrialized countries, and its morbidity increases among school-aged children [1, 2]. A survey conducted from 1987 to 2013 in mainland China indicated that the prevalence of early childhood caries reached 63.5% in rural areas and 59.5% in urban areas [3]. Anaerobic oral microorganisms mainly cause dental caries because they can produce acids through glycometabolism and these acids demineralize the tooth enamel and finally resulting in the onset of the disease [4]. *Streptococcus mutans* (*S. mutans*) is the most potent cariogenic bacteria and is closely implicated in every type of dental caries [5, 6]. Effective control of *S. mutans* is critical in the prevention and treatment of oral diseases.

Recent studies have indicated that nanotechnology can provide novel strategies in prevention and treatment of dental caries, especially in the control of oral pathogenic bacteria [7]. Zinc oxide (ZnO) has been widely used in clinics as dental materials, such as endodontic sealers and fixed restoration cement, because of its high biocompatibility and ability to sterilize [8], which is already recognized by the U.S. Food and Drug Administration [(21CFR182.8991) (FDA, 2011)] [9]. Nano-sized ZnO can be incorporated into dental composites to improve the antibacterial capacity of these dental materials [10, 11].

However, the antibacterial activity of ZnO nanoparticles (NPs) is limited, in which ZnO NPs exert effects against *S. mutans* only at high concentrations [12]. When large amounts of ZnO NPs are incorporated into dental composites, the physical and mechanical properties of the composites may change. Similar to ZnO NPs, Ag NPs show antibacterial effects against several types of bacteria,

including *S. mutans* [13–16]. Furthermore, Ag NPs have been incorporated into dental materials to combat cariogenic bacteria, and they display a considerably higher antibacterial activity than ZnO NPs [17]. However, a number of evidence has proven the cytotoxicity and genotoxicity of Ag NPs to human cells [18, 19]. In using Ag safely, the amount of Ag NPs can be effectively reduced by supporting them on ZnO without jeopardizing their functionality. In addition, Ag/ZnO nanocomposite can synergistically inhibit the bacteria due to the interaction between Ag and ZnO [20–23]. The antibacterial activity of Ag/ZnO nanocomposite against Gram-positive (*Staphylococcus aureus* and *Bacillus subtilis*) and Gram-negative bacteria (*Escherichia coli*) has been demonstrated [20, 23]. However, the efficacy of Ag/ZnO nanocomposite against oral pathogens, most of which are anaerobic and facultative anaerobic bacteria, has not yet been reported. For this reason, this study evaluated the antibacterial activities of Ag/ZnO nanocomposite against *S. mutans* and compared these activities with those of ZnO NPs. The disruption of membrane function and generation of intracellular reactive oxygen and lipid peroxidation induced by Ag/ZnO nanocomposite were measured using different assays to investigate the antibacterial mechanism of this nanocomposite.

2 Materials and methods

2.1 Materials

Zinc acetate dehydrate ($Zn(CH_3COO)_2{\cdot}2H_2O$) was purchased from Sinopharm Chemical Reagent Co., Ltd. (China). Sodium hydroxide (NaOH), silver nitrate ($AgNO_3$) and thiobarbituric acid (TBA) were purchased from Aladdin (China). 3, 3'-dipropylthiacarbocyanine iodide ($DiSC_35$) and 2, 7-dichlorofluorescein diacetate (DCFH-DA) were purchased from Sigma-Aldrich (USA). Trichloroacetic acid (TCA) was purchased from Tianjin Kemiou Chemical Reagent Co., Ltd.

The bacteria strains of *S. mutans* (Ing.bitt) was obtained from School of Stomatology, Wuhan University and grown aerobically at 37 °C in brain heart infusion (BHI) medium (Oxoid, England).

2.2 Preparation of Ag/ZnO nanocomposite

ZnO nanorods were prepared via a solvothermal method [24]. Typically, 1 mmol $Zn(CH_3COO)_2{\cdot}2H_2O$ and 10 mmol NaOH were dissolved in 30 mL absolute ethyl alcohol, then the mixture was transferred to a Teflon liner stainless steel autoclave to perform a solvothermal process at 150 °C for 24 h. After cooling down to room temperature, the product was collected by centrifugation and washed with deionized water and alcohol for five times, then dried in a oven at 60 °C overnight to obtain ZnO nanorods.

The deposition-precipitation method was used to prepare Ag/ZnO nanocomposite. Typically, 0.1 g of as-prepared ZnO was dispersed in 12.5 mL of $AgNO_3$ solution (10 mmol/L) under sonication. Then the mixture was heated to 80 °C, followed by adjusting pH to 8 using NaOH solution, and continued to stir at 80 °C for 4 h in the dark. After cooling down to room temperature, the product was collected by centrifugation and washed with deionized water for three times, then dried in a desiccator at room temperature to obtain Ag/ZnO nanocomposite with 10% Ag molar content.

X-ray diffraction (XRD) measurement was carried on Bruker axs D8 Discover (Cu $K_\alpha = 1.5406$ Å). Morphology and size of the products were characterized by scanning electron microscope (SEM, Hitachi S4800, operating at 5 eV) and transmission electron microscope (TEM, Philips Tecnai 20, operating at an accelerating voltage of 200 kV). Inductively coupled plasma-atomic emission spectrometry (ICP-AES, IRIS Intrepid IIXSP, Perkin Elmer) was used to determine the composite of Ag/ZnO nanocomposite. The zeta potential of synthesized sample was measured by Malvern laser particle size analyzer (Nano ZS90).

2.3 Antibacterial activity test

Inhibitory efficacy of ZnO and Ag/ZnO nanomaterials against *S. mutans* was evaluated by determining the values of minimal inhibitory concentration (MIC) and minimum bactericidal concentration (MBC) as well as growth inhibition curve. Briefly, aliquots of 50 µL of 10^5 CFU/mL bacteria suspension were mixed with 50 µL of serially diluted ZnO or Ag/ZnO nanomaterials in 96-well plate and the mixture was incubated at 37 °C for 24 h under microaerobic conditions. The lowest concentration of the nanomaterials that resulted in no visible turbidity was considered as the MIC [25]. Further spreading 10 µL of the culture from the well which seemed clarity on BHI agar plate and incubated at 37 °C for 24 h, then the number of the colonies were counted. The MBC value is defined as the concentration of the antibacterial agent that causes more than 99.9% bacterial population killed [26].

The inhibition on growth cure was determined by mixing 50 µL of 10^5 CFU/mL bacteria suspension with 50 µL of 512 µg/mL ZnO or Ag/ZnO nanomaterials and incubated at 37 °C for 24 h. The optical density (OD) values at 600 nm was recorded by a microplate reader (RT-6000, Rayto) every 2 h. A blank without nanomaterials were served as control. All experiments were repeated three times.

2.4 Observation of the bacterial morphology

The mixture of 2 mL of 256 μg/mL nanomaterials with 2 mL of 10^5 CFU/mL *S. mutans* was incubated at 37 °C for 8 h, then centrifuged and washed the precipitate with PBS buffer. After fixing with 2.5% glutaraldehyde at 4 °C for 2 h, the samples were dehydrated with a grade ethanol solutions. Cells were gold sprayed and imaged by a field-emission scanning electron microscopy (FE-SEM, Quanta 450 FEG) at an extra high tension of 5.0 kV. Culture without nanomaterial served as control.

2.5 Membrane potential assay

Membrane potential assay was performed according to the established procedure using the membrane potential probe $DiSC_35$ [27]. Firstly, the 10^7 CFU/mL bacteria suspension was incubated with 0.4 μmol/L of $DiSC_35$ for 1 h. Then immediately ion-equilibrated with 4 mol/L KCl for 1 h. After that, 256 μg/mL nanomaterials were added into the above bacteria suspension and incubated at 37 °C for 1 h, then the fluorescence was monitored with excitation at 622 nm and emission at 670 nm by a spectrofluorophotometer (Hitachi F4600).

2.6 Leakage of K^+

S. mutans cells were suspended in 2.5 mmol/L HEPES buffer (pH 7.0) containing 10 mmol/L glucose to the concentration of 10^8 CFU/mL. After 1 h treatment with 256 μg/mL of ZnO or Ag/ZnO nanomaterials, the mixture was centrifuged and the supernatant was collected, then the concentration of K^+ was determined by inductively coupled plasma-mass spectrometry (ICP-MS, PerkinElmer NexION 300X) [28].

2.7 Intracellular reactive oxygen species (ROS)

Intracellular ROS was monitored with an oxidation-sensitive fluorescent probe DCFH-DA. After incubation of *S. mutans* (10^8 CFU/mL) with 512 μg/mL ZnO or Ag/ZnO nanomaterials at 37 °C for 5 h, cells suspension was incubated with 100 μmol/L DCFH-DA at 37 °C for 1 h. Then the bacteria cells were pelleted by centrifugation and washed two times with PBS. The fluorescence intensity was measured by a fluorescence spectrophotometer at excitation and emission of 450 and 535 nm, respectively.

2.8 Lipid peroxidation

To determine the effect of ZnO and Ag/ZnO nanomaterials on lipid peroxidation of bacteria, 512 μg/mL ZnO or Ag/ZnO nanomaterials was mixed with equal value *S. mutans* (10^6 CFU/mL) and incubated at 37 °C overnight, then added equal value 10% ice-cold TCA and further incubated for 20 min. The mixture was centrifuged at 1000 rpm for 10 min, then 1 mL of 0.6% TBA was added to 1 mL of supernatant and boiled for 2 h. The sample was cooled to room temperature, and the absorbance at 535 nm was determined by UV/visible spectrophotometer (UV 4500, Perkin Elmer).

3 Results

3.1 Morphology and structure of Ag/ZnO sample

The as-prepared products characterized by powder XRD are shown in Fig. 1a. All diffraction peaks of the as-prepared ZnO could be perfectly indexed to the hexagonal wurtzite phase of ZnO (JCPDS 36-1451) with no impurity diffraction peaks detected, indicating the high purity of ZnO products. In additional to ZnO diffraction peaks, there are some peaks observed in the XRD patterns of the Ag/ZnO products at $2\theta = 38.1°$, 44.3°, and 64.4°, which are corresponding to the pattern of Ag (JCPDS 04-0783), demonstrating the production of Ag/ZnO. The morphology and structure of the as prepared ZnO and Ag/ZnO were characterized by SEM and TEM. As shown in Fig. 1b, c, both of the products exhibits rod-like morphology with length of 300~500 nm and width of 10~20 nm. The TEM image in Fig. 1d illustrates the successful dispersion of 15 nm Ag nanoparticles on ZnO surface. The chemical composition of Ag/ZnO nanocomposite was also analyzed by ICP-AES and the molar percentages of Ag element in Ag/ZnO is 7.04%. The zeta potential of ZnO and Ag/ZnO nanomaterials are 25.29 and 14.0 mV, respectively.

3.2 Antibacterial activity of Ag/ZnO nanocomposite

The antimicrobial activity of Ag/ZnO nanocomposite against oral anaerobic pathogenic *S. mutans* assessed by determining the values of MIC and MBC is shown in Table 1. It is seen that the MIC and MBC of the Ag/ZnO nanocomposite are obviously lower than that of ZnO nanorods, which demonstrates the higher antibacterial activity of Ag/ZnO nanocomposite.

The inhibitory effect of Ag/ZnO nanocomposite on *S. mutans* growth is shown in Fig. 2. It is observed that both ZnO and Ag/ZnO nanomaterials obviously delayed the progress of bacteria to logarithmic growth and cut down the number of bacteria. At the concentration of 256 μg/mL, Ag/ZnO nanocomposite inhibited 91% of bacteria growth after 24 h of incubation. However, ZnO nanorods only reduced 50% of bacteria growth. These results demonstrate that the incorporation of Ag in ZnO nanorods can highly increase the antibacterial activity of ZnO nanorods.

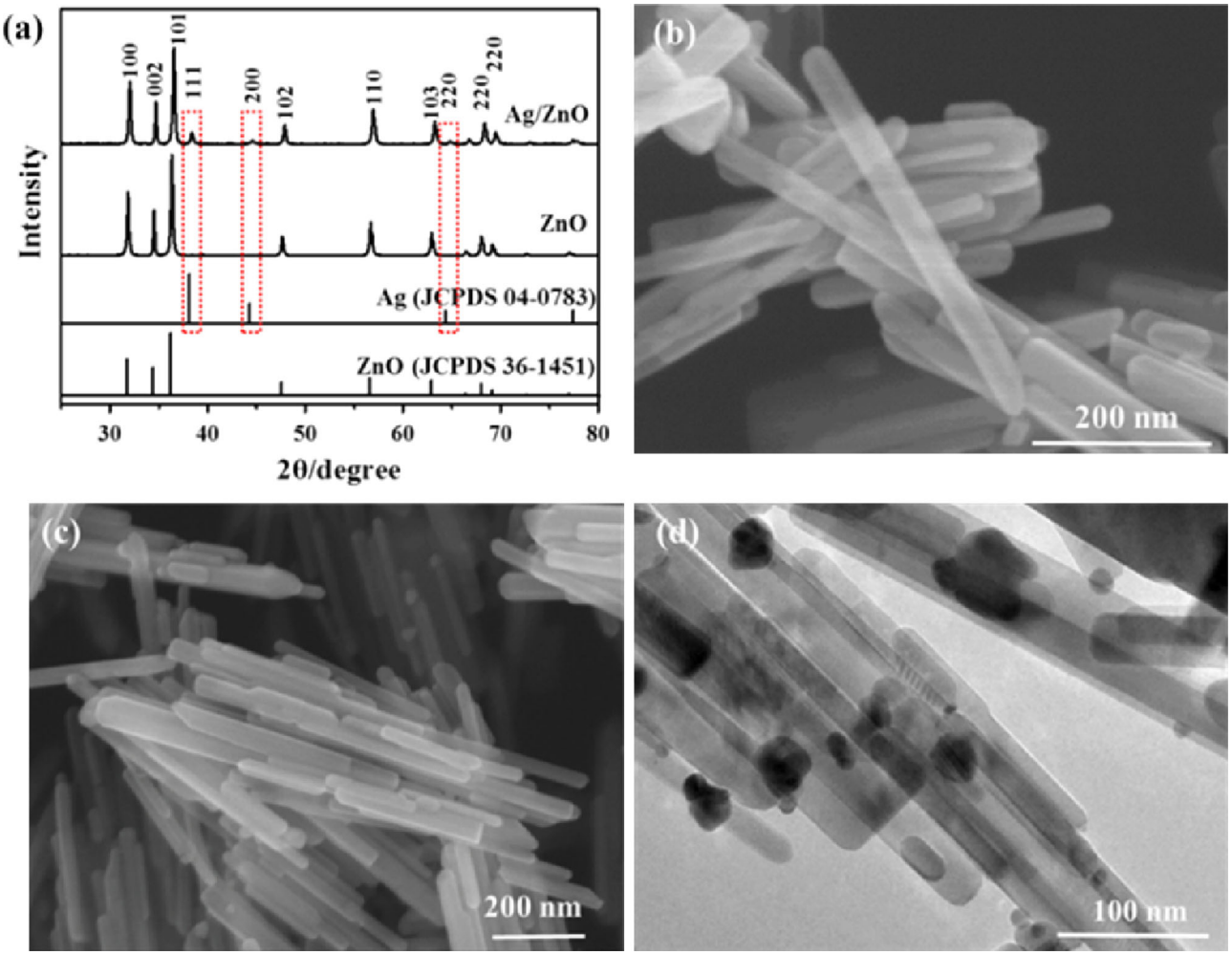

Fig. 1 XRD patterns (**a**), SEM image of ZnO nanorods (**b**) and Ag/ZnO nanocomposite (**c**), and TEM image of Ag/ZnO nanocomposite (**d**)

Table 1 The MIC and MBC values of ZnO and Ag/ZnO nanomaterials against *S. mutans*

Antimcrobials	MIC (μg/mL)	MBC (μg/mL)
ZnO	512	>1024
Ag/ZnO	256	512

3.3 Bacteria morphology observation

The morphology of *S. mutans* treated by ZnO or Ag/ZnO nanomaterials was observed by FE-SEM and shown in Fig. 3. Untreated *S. mutans* cells have a spherical-like morphology and a relatively smooth surface (Fig. 3a). After 8 h of treatment with 128 μg/mL of ZnO nanorods, the bacteria cells collapsed and some intracellular content released (Fig. 3b). However, the most damaged cells are observed by Ag/ZnO nanocomposite treatment (Fig. 3c, d). The membrane of *S. mutans* scattered and the sphere-like morphology of bacteria cell became almost disorganized.

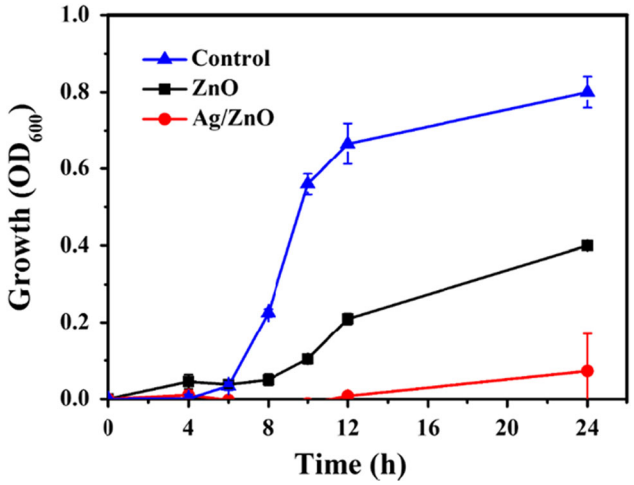

Fig. 2 Growth curves of *S. mutans* incubated with ZnO or Ag/ZnO nanomaterials

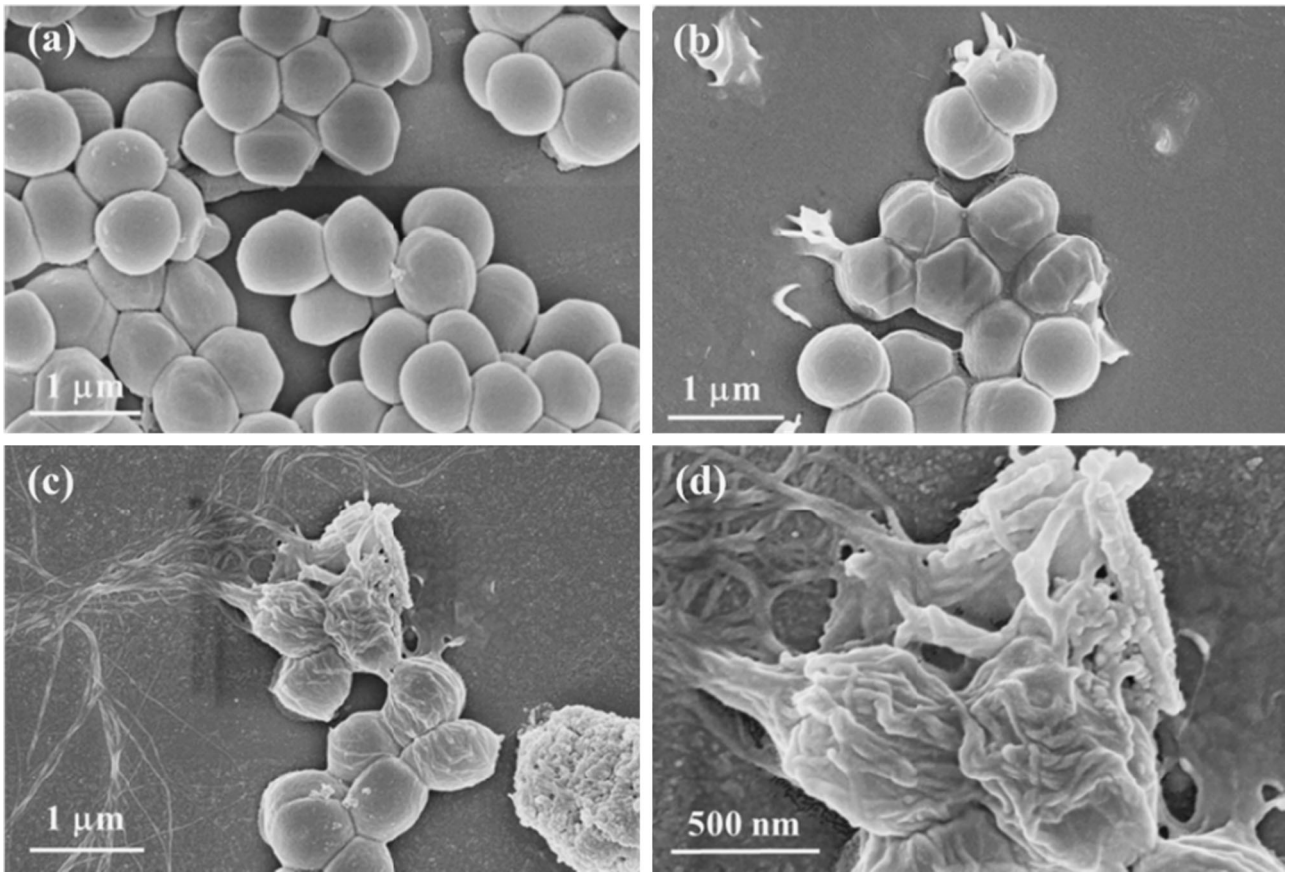

Fig. 3 FE-SEM images of untreated *S. mutans* (**a**) and treated by ZnO nanorods (**b**) and Ag/ZnO nanocomposite (**c**, **d**)

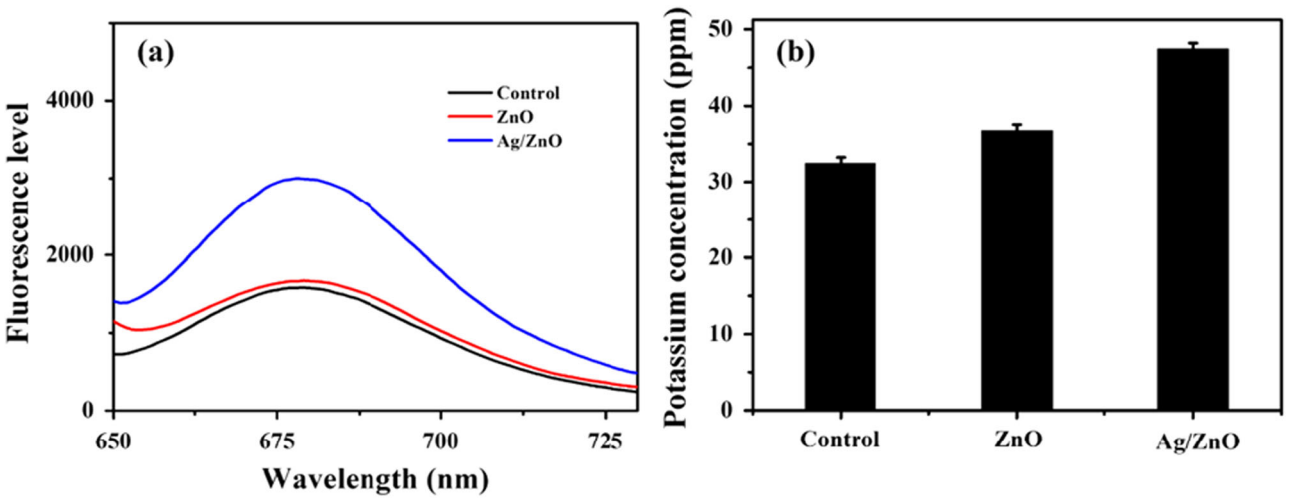

Fig. 4 Effects of Ag/ZnO nanocomposite on *S. mutans* membrane properties. **a** Membrane potential probed with the $DiSC_35$ dye; **b** Concentration of potassium in culture medium

3.4 Effect of Ag/ZnO nanocomposite on membrane properties of *S. mutans*

The bacterial cell membrane serves as a barrier between cytoplasm and extracellular medium. It is known that the disruption of the membrane can cause the membrane depolarization [28]. In order to determine whether Ag/ZnO nanocomposite affected the membrane function of *S. mutans*, the effect of Ag/ZnO nanocomposite at MIC on the cytoplasmic membrane potential of *S. mutans* was

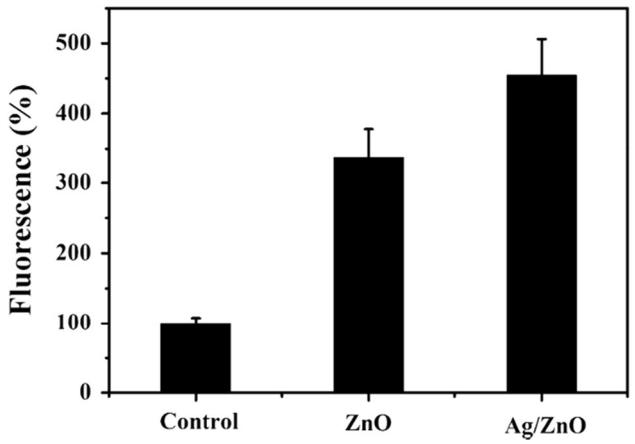

Fig. 5 Intracellular ROS generation after ZnO and Ag/ZnO nanomaterials treatment

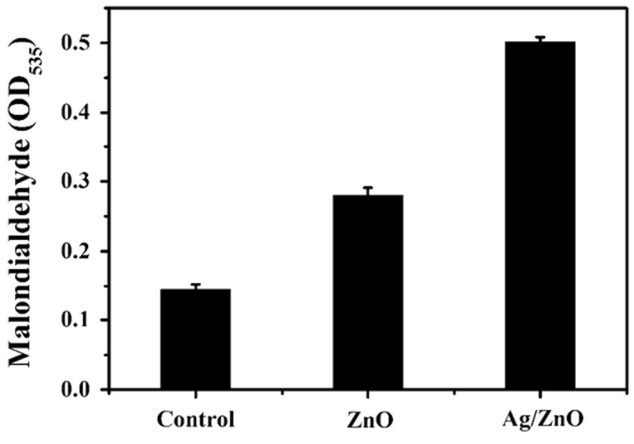

Fig. 6 Lipid peroxidation in *S. mutans* after ZnO and Ag/ZnO treatment

examined using fluorescence probe $DiSC_35$ [29]. The fluorescent probe $DiSC_35$ will accumulate inside bacterial cells, unless the cytoplasmic membrane is permeabilized and caused a measurable increase in fluorescence level [30]. As shown in Fig. 4a the addition of Ag/ZnO nanocomposite resulted in a highly increased of fluorescence, indicative of a dissipation of the membrane potential. The addition of ZnO nanorods at the same concentration caused small increase in fluorescence, which demonstrated the lower destructive effect of ZnO nanorods on the membrane of *S. mutans* cells.

To further verify the change of the permeability of *S. mutans* cell membrane, we examined the effects of Ag/ZnO nanocomposite on the release K^+ ions from cells. As shown in Fig. 4b, after 1 h of incubation, both ZnO and Ag/ZnO nanomaterials added at 256 μg/mL resulted in an obvious increase of K^+ ions concentration in culture medium, indicative of a disruption of the membrane. Furthermore, Ag/ZnO nanocomposite caused higher K^+ ions release than ZnO nanorods.

3.5 Intracellullar ROS generation

In order to investigate if ROS is associated with the antibacterial action of Ag/ZnO, the intracellular ROS generation after ZnO and Ag/ZnO treatment was determined by DCFH-DA fluorescent probe and shown in Fig. 5. DCFH-DA, an oxidation-sensitive fluorescent probe, can confirm the intracellular ROS. It can cross the cell membrane into the cell and hydrolyzes by intracellular esterase to non-fluorescent DCFH. In the presence of ROS, DCFH is oxidized to highly fluorescent dichlorofluorescein (DCF) [31]. It is seen that the fluorescence intensity for Ag/ZnO nanocomposite treated cells is about 4.5-fold increase compared to untreated control, while pure ZnO nanorods with the same concentration caused about 3.4-fold increase. These results indicated that more intracellular ROS was generated after ZnO and Ag/ZnO nanomaterials treatment and Ag/ZnO possessed most ROS generation.

3.6 ROS-mediated lipid peroxidation injury

In order to confirm ROS-related oxidative injury, lipid peroxidation of bacteria was detected by assaying for malondialdehyde (MDA) and shown in Fig. 6. It is seen that the addition of Ag/ZnO nanocomposite significantly increased the concentration of MDA in *S. mutans*, indicative of the oxidative injury caused by Ag/ZnO nanocomposite. It is also seen that Ag/ZnO nanocomposite caused more oxidative injury than ZnO nanorods at the same concentration.

4 Discussion

Dental caries is one of the most common infectious diseases in humans. If untreated, dental caries will generate carious cavity and further destroy the dental crown. Although oral micro-ecosystem consists of more than one hundred known bacteria, *S. mutans* remains to be the primary pathogenic microorganism in caries [5]. Despite continuous efforts in the pharmaceutical industry to develop effective antibacterial agents, increasing resistance of microorganisms to common antibiotics has become an important concern [32]. Searching for new broad-spectrum drugs to fight antimicrobial resistance is urgently needed. Studies have shown that Ag and ZnO nanomaterials exhibit a broad-spectrum antimicrobial activity against bacteria [33, 34]. However, Ag nanoparticles are not suitable for long-term storage and high dosage of which is considerably toxic to humans [19, 35]. Although ZnO NPs are not as toxic as Ag NPs, their antibacterial activity is comparatively lower [19]. To address these problems, we incorporated Ag NPs into ZnO

nanorods to form Ag/ZnO nanocomposite by using the deposition-precipitation method (Fig. 1). Ag/ZnO nanocomposite showed higher antibacterial activity than ZnO nanorods (Table 1) and obviously delayed the growth of *S. mutans* (Fig. 2) with much lower Ag molar ratio (7.04%).

For aerobic microorganisms, disruption of membrane function and ROS-related oxidative injury are commonly associated with the antibacterial action of inorganic nanomaterials [21, 23]; however, the antibacterial mechanisms of Ag/ZnO against anaerobic *S. mutans* have not yet been explored. We first intensively analyzed the bacterial morphology after Ag/ZnO nanocomposite treatment by using FE-SEM (Fig. 3). Ag/ZnO nanocomposite induced more severe physical damage in bacteria than ZnO nanorods. Compared with some of the reported ZnO and Ag/ZnO nanomaterials [36, 37], our ZnO and Ag/ZnO nanomaterials both showed positive zeta potential, which is beneficial for the nanomaterials to approach bacterial cells and adsorb to electronegative cell surface.

Che et al. [37] reported that nano-Ag destabilizes the outer membrane and disrupts the plasma membrane potential of the aerobic bacteria *E.coli*. We observed similar result, wherein Ag/ZnO nanocomposite disrupted the membrane potential of anaerobic *S. mutans* (Fig. 4a). Disruption of the bacterial membrane function by Ag/ZnO nanocomposite was further confirmed by the release of K^+ from the cytoplasm. A high intracellular concentration of K^+ mediated by inward flux largely maintains the membrane potential of bacteria [29]; therefore, the release of large amounts of K^+ from the cytoplasm reflects the collapse of membrane function caused by Ag/ZnO nanocomposite (Fig. 4b). We deduced based on these results that the disrupted membrane function probably led to the death of *S. mutans,* consistent with the mechanisms of some inorganic nano-antibacterial agents (e.g., Ag and AuPt) against aerobic bacteria [38].

Studies have reported that intracellular ROS production is highly associated with the antibacterial effect of nanoparticles [23, 39]. Hui et al. [39] found that H_2O_2 production in ZnO suspension is responsible for the antibacterial effect of ZnO against *E. coli*. Moreover, Zhang et al. [23] reported that Ag/ZnO heterostructure nanoparticles can induce increased cellular ROS generation in *S. aureus* and *E. coli*. However, whether ROS production contributes to the antibacterial activity of Ag/ZnO nanoparticles against *S. mutans* remains unknown. This study used DCFH-DA as a visual indicator to determine the presence of ROS in a bacteria cell. Our results confirmed that Ag/ZnO nanocomposite could increase intracellular ROS generation (Fig. 5). Lipid peroxidation is a signature of ROS damage in bacteria and can be detected by assaying malondialdehyde (MDA), an oxidized product of polyunsaturated fatty acid [36]. *S. mutans* exposed to Ag/ZnO nanocomposite showed increased MDA concentration (Fig. 6), indicating a considerable oxidative damage in cells caused by Ag/ZnO. Our results confirmed that intracellular ROS generation played an important role in antibacterial action of Ag/ZnO nanocomposite against anaerobic *S. mutans.*

5 Conclusion

Ag/ZnO nanocomposite was successfully synthesized using the deposition-precipitation method. Compared with ZnO nanorods, Ag/ZnO nanocomposite showed enhanced antibacterial activity against the oral anaerobic pathogenic *S. mutans.* The antibacterial mechanism involves the direct destruction of cell structure and membrane function, as well as the generation of ROS to oxidize biomacromolecules. The results demonstrate the potential application of the prepared Ag/ZnO nanocomposite in dentistry.

Acknowledgements This work was supported by National Natural Science Foundation of China (21371139, 21201135), Graduate Innovative Found of Wuhan Institute of Technology (CX2015139) and High-Tech Industry Technology Innovation Team Training Program of Wuhan Science and Technology Bureau (20140704020243).

Compliance with Ethical Standards

Conflict of interest The authors declare no competing financial interests.

References

1. Bagramian RA, Garcia-Godoy F, Volpe AR. The global increase in dental caries. A pending public health crisis. Am J Dent. 2009;21:3–8.
2. Petersen PE, Bourgeois D, Ogawa H, Estupinan-Day S, Ndiaye C. The global burden of oral diseases and risks to oral health. Bull World Health Organ. 2005;83:661–9.
3. Zhang X, Yang S, Liao Z, Xu L, Li C, Zeng H, Song J, Zhang L. Prevalence and care index of early childhood caries in mainland China: evidence from epidemiological surveys during 1987-2013. Sci Rep. 2016;6:18897
4. He J, Wang S, Wu T, Cao Y, Xu X, Zhou X. Effects of ginkgoneolic acid on the growth, acidogenicity, adherence, and biofilm of *Streptococcus mutans* in vitro. Folia Microbiol (Praha). 2013;58:147–53.
5. Loesche WJ. Role of *Streptococcus mutans* in human dental decay. Microbiol Rev. 1986;50:353–80.
6. Hasan S, Danishuddin M, Khan AU. Inhibitory effect of zingiber officinale towards *Streptococcus mutans* virulence and caries development: in vitro and in vivo studies. BMC Microbiol. 2015;15:1
7. Padovani GC, Feitosa VP, Sauro S, Tay FR, Duran G, Paula AJ, Duran N. Advances in dental materials through nanotechnology: facts, perspectives and toxicological aspects. Trends Biotechnol. 2015;33:621–36.
8. Javidi M, Zarei M, Naghavi N, Mortazavi M, Nejat AH. Zinc oxide nano-particles as sealer in endodontics and its sealing ability. Contemp Clin Dent. 2014;5:20–4.

9. Jin T, Sun D, Su JY, Zhang H, Sue HJ. Antimicrobial efficacy of zinc oxide quantum dots against listeria monocytogenes, salmonella enteritidis, and escherichia coli O157:H7. J Food Sci. 2009;74:M46–52.
10. Allaker RP. The use of nanoparticles to control oral biofilm formation. J Dent Res. 2010;89:1175–86.
11. Sevinc BA, Hanley L. Antibacterial activity of dental composites containing zinc oxide nanoparticles. J Biomed Mater Res B. 2010;94:22–31.
12. Eshed M, Lellouche J, Matalon S, Gedanken A, Banin E. Sonochemical coatings of ZnO and CuO nanoparticles inhibit *Streptococcus mutans* biofilm formation on teeth model. Langmuir. 2012;28:12288–95.
13. Freire PLL, Stamford TCM, Albuquerque AJR, Sampaio FC, Cavalcante HMM, Rui OM, Galembeck A, Flores MAP, Rosenblatt A. Action of silver nanoparticles towards biological systems: cytotoxicity evaluation using hen's egg test and inhibition of *Streptococcus mutans* biofilm formation. Int J Antimicrob Ag. 2015;45:183–7.
14. Lu Z, Rong K, Li J, Yang H, Chen R. Size-dependent antibacterial activities of silver nanoparticles against oral anaerobic pathogenic bacteria. J Mater Sci Mater Med. 2013;24:1465–71.
15. Li J, Rong K, Zhao H, Li F, Lu Z, Chen R. Highly selective antibacterial activities of silver nanoparticles against *Bacillus subtilis*. J Nanosci Nanotechnol. 2013;13:6806–13.
16. Sharma VK, Yngard RA, Lin Y. Silver nanoparticles: green synthesis and their antimicrobial activities. Adv Colloid Interface Sci. 2009;145:83–96.
17. Vargas-Reus MA, Memarzadeh K, Huang J, Ren GG, Allaker RP. Antimicrobial activity of nanoparticulate metal oxides against peri-implantitis pathogens. Int J Antimicrob Agents. 2012;40:135–9.
18. Li L, Sun J, Li X, Zhang Y, Wang Z, Wang C, Dai J, Wang Q. Controllable synthesis of monodispersed silver nanoparticles as standards for quantitative assessment of their cytotoxicity. Biomaterials. 2012;33:1714–21.
19. Asharani PV, Mun GLK, Hande MP, Valiyaveettil S. Cytotoxicity and genotoxicity of silver nanoparticles in human cells. ACS Nano. 2009;3:279–90.
20. Agnihotri S, Bajaj G, Mukherji S, Mukherji S. Arginine-assisted immobilization of silver nanoparticles on ZnO nanorods: an enhanced and reusable antibacterial substrate without human cell cytotoxicity. Nanoscale. 2015;7:7415–29.
21. Matai I, Sachdev A, Dubey P, Kumar SU, Bhushan B, Gopinath P. Antibacterial activity and mechanism of Ag-ZnO nanocomposite on *S. aureus* and GFP-expressing antibiotic resistant *E. coli*. Colloid Surf B. 2014;115:359–67.
22. Patil SS, Patil RH, Kale SB, Tamboli MS, Ambekar JD, Gade WN, Kolekar SS, Kale BB. Nanostructured microspheres of silver @ zinc oxide: an excellent impeder of bacterial growth and biofilm. J Nanopart Res. 2014;16:1–11.
23. Zhang Y, Gao X, Zhi L, Liu X, Jiang W, Sun Y, Yang J. The synergetic antibacterial activity of Ag islands on ZnO (Ag/ZnO) heterostructure nanoparticles and its mode of action. J Inorg Biochem. 2014;130:74–83.
24. Wang Q, Geng B, Wang S. ZnO/Au hybrid nanoarchitectures: wet-chemical synthesis and structurally enhanced photocatalytic performance. Environ Sci Technol. 2009;43:8968–73.
25. Espinosa-Cristóbal LF, Martínez-Castañón GA, Martínez-Martínez RE, Loyola-Rodríguez JP, Patiño-Marín N, Reyes-Macías JF, Ruiz F. Antimicrobial sensibility of *Streptococcus mutans* serotypes to silver nanoparticles. Mater Sci Eng C. 2012;32:896–901.
26. Wang HY, Cheng JW, Yu HY, Lin L, Chih YH, Pan YP. Efficacy of a novel antimicrobial peptide against periodontal pathogens in both planktonic and polymicrobial biofilm states. Acta Biomater. 2015;25:150–61.
27. Zhang L, Scott MG, Yan H, Mayer LD, Hancock RE. Interaction of polyphemusin I and structural analogs with bacterial membranes, lipopolysaccharide, and lipid monolayers. Biochemistry. 2000;39:14504–14.
28. Zhou K, Zhou W, Li P, Liu G, Zhang J, Dai Y. Mode of action of pentocin 31-1: An antilisteria bacteriocin produced by *Lactobacillus pentosus* from Chinese traditional ham. Food Control. 2008;19:817–22.
29. Lok CN, Ho CM, Chen R, He QY, Yu WY, Sun H, Tam PK, Chiu JF, Che CM. Proteomic analysis of the mode of antibacterial action of silver nanoparticles. J Proteome Res. 2006;5:916–24.
30. Kuwano K, Tanaka N, Shimizu T, Nagatoshi K, Nou S, Sonomoto K. Dual antibacterial mechanisms of nisin Z against gram-positive and gram-negative bacteria. Int J Antimicrob Agents. 2005;26:396–402.
31. Ghosh S, Saraswathi A, Indi SS, Hoti SL, Vasan HN. Ag@AgI, core@shell structure in agarose matrix as hybrid: synthesis, characterization, and antimicrobial activity. Langmuir. 2012;28:8550–61.
32. Chastre J. Evolving problems with resistant pathogens. Clin Microbiol Infect. 2008;14(Suppl 3):3–14.
33. Guzman M, Dille J, Godet S. Synthesis and antibacterial activity of silver nanoparticles against gram-positive and gram-negative bacteria. Nanomedicine. 2012;8:37–45.
34. Seil JT, Webster TJ. Antibacterial effect of zinc oxide nanoparticles combined with ultrasound. Nanotechnology. 2012;23:6690–700.
35. Li X, Lenhart JJ. Aggregation and dissolution of silver nanoparticles in natural surface water. Environ Sci Technol. 2012;46:5378–86.
36. Eshed M, Lellouche J, Gedanken A, Banin E. A Zn-doped CuO nanocomposite shows enhanced antibiofilm and antibacterial activities against *Streptococcus mutans* compared to nanosized CuO. Adv Funct Mater. 2014;24:1382–90.
37. Lin D, Wu H, Zhang R, Pan W. Enhanced photocatalysis of electrospun Ag–ZnO heterostructured nanofibers. Chem Mater. 2009;21:3479–84.
38. Zhao Y, Ye C, Liu W, Chen R, Jiang X. Tuning the composition of AuPt bimetallic nanoparticles for antibacterial application. Angew Chem Int Ed Engl. 2014;53:8127–31.
39. Xu X, Chen D, Yi Z, Jiang M, Wang L, Zhou Z, Fan X, Wang Y, Hui D. Antimicrobial mechanism based on H_2O_2 generation at oxygen vacancies in ZnO crystals. Langmuir. 2013;29:5573–80.